THE JOURNAL OF PHYSICAL CHEMISTRY A
A JOURNAL OF THE AMERICAN CHEMICAL SOCIETY

pubs.acs.org/JPCA Article

Efficient Method for an Approximate Treatment of the Coriolis Effect in Calculations of Quantum Dynamics and Spectroscopy, with Application to Scattering Resonances in Ozone

Igor Gayday and Dmitri Babikov*

Cite This: *J. Phys. Chem. A* 2021, 125, 5661−5669 Read Online

ACCESS | Metrics & More | Article Recommendations | Supporting Information

ABSTRACT: A numerical approach is developed to capture the effect of rotation−vibration coupling in a practically affordable way. In this approach only a limited number of adjacent rotational components are considered to be coupled, while the couplings to other rotational components are neglected. This partially coupled (PC) approach permits to reduce the size of Hamiltonian matrix significantly, which enables the calculations of ro-vibrational states above dissociation threshold (scattering resonances) for large values of total angular momentum. This method is employed here to reveal the role of the Coriolis effect in the ozone formation reaction at room temperature, dominated by large values of total angular momentum states, on the order of J = 24 and 28. We found that, overall, the effect of ro-vibrational coupling is not minor for large J. Compared to the results of symmetric top rotor approximation, where the ro-vibrational coupling is neglected, we found that the widths of scattering resonances, responsible for the lifetimes of metastable ozone states, remain nearly the same (on average), but the number of these states increases by as much as 20%. We also found that these changes are nearly the same in symmetric and asymmetric ozone isotopomers $^{16}O^{18}O^{16}O$ and $^{16}O^{16}O^{18}O$. Therefore, based on the results of these calculations, the Coriolis coupling does not seem to favor the formation of asymmetric ozone molecules and thus cannot be responsible for symmetry-driven mass-independent fractionation of oxygen isotopes.

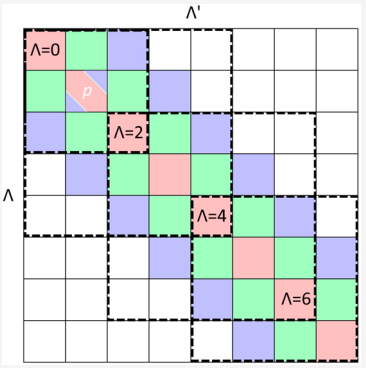

I. INTRODUCTION

Accurate variational calculations of rotational−vibrational states of molecules involve diagonalization of huge Hamiltonian matrices that contain up to J + 1 diagonal blocks (corresponding to the symmetric-top rotor states), coupled by the off-diagonal blocks that appear due to the asymmetric-top rotor and Coriolis terms.[1] Numerically accurate implementation of such full-coupled treatment is considered to be exact, but it is computationally demanding and is therefore feasible for the simplest cases only, such as sparce spectra of molecules with large rotational constants and/or low levels or rotational and vibrational excitations. Several examples of the fully coupled calculations are available from recent literature for small values of total angular momentum.[2−5] Usually, such calculations aim at the spectroscopic applications, where a stable (bound) molecule is vibrating in the vicinity of equilibrium configuration.

However, there are other important applications where a brute force diagonalization of the entire Hamiltonian matrix is numerically unaffordable, even with the fastest supercomputers available to us today. For example, it is challenging to carry out the variational calculations of vibrational states up to dissociation threshold, where the large-amplitude floppy motion is typical, and this becomes even more difficult if a broad range of angular momentum states is needed (e.g., for calculations of thermally averaged moieties). One application that we consider below concerns calculations of scattering resonances *above* the dissociation threshold, on a potential energy surface (PES) with complicated landscape, where several isotopomers are present at the same time, at large value of total angular momentum (around J = 25−30), for a molecule with small rotational constants. For this purpose, we developed and tested an approximate method to take into account the effects of rotation−vibration coupling, which remains practical even in this and other complicated cases.

In our method, instead of diagonalization of the entire Hamiltonian matrix as a whole, we run a series of independent calculations for all needed values of the symmetric-top quantum number (i.e., z-projection of the total angular momentum, here denoted Λ) in the range $0 \le \Lambda \le J$. In each of these runs, we diagonalize a reduced matrix, which includes only the blocks coupled directly to a given value of Λ,

Received: April 13, 2021
Revised: June 8, 2021
Published: June 22, 2021

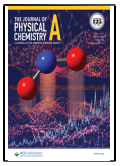

https://doi.org/10.1021/acs.jpca.1c03350
J. Phys. Chem. A 2021, 125, 5661−5669

which is $\Lambda \pm 2$ at most. Therefore, each individual calculation includes no more than five Λ-blocks, which permits to capture the major effect of the rotation−vibration coupling terms, while keeping the cost of calculations practical.

Indeed, the cost of matrix diagonalization grows at least quadratically. Therefore, replacing one diagonalization of a matrix that contains $(J + 1) \times (J + 1)$ blocks with a series of $J + 1$ independent diagonalizations of the matrices that contain 5 × 5 blocks at most, one can gain a substantial computational advantage. Interestingly, a similar idea was recently developed in the context of a nonreactive inelastic scattering and was found to be both accurate and numerically efficient.[6] We would like to call this approach a *partially coupled* method, or a PC-method for short, to complement the well-known coupled-channel (CC), centrifugal-sudden (CS), and infinite-order sudden (IOS) methods.[7−10]

This approach helps to answer a tough question about the role of Coriolis coupling in the recombination reaction that forms ozone. It is well-known[12] that isotopically substituted asymmetric ozone molecules, such as $^{18}O^{16}O^{16}O$, are formed faster than symmetric ozone molecules, such as $^{16}O^{18}O^{16}O$ or $^{16}O^{16}O^{16}O$. This leads to the mass-independent enrichment of atmospheric ozone in the rare isotopes of oxygen, which is an important natural phenomenon with multiple implications in atmospheric chemistry, geoscience, and planetary science.[13,14] The molecular level explanation of this isotope effect is still missing, but one popular hypothesis, suggested by Marcus and co-workers,[15,16] claims that some of the Coriolis coupling terms may be absent in symmetric ozone molecules but be present in the asymmetric ones, leading to a symmetry-driven (rather than mass-driven) isotope effect. To check this hypothesis, they performed classical simulations of the "diffusion" of vibrational excitations through the rotational states of symmetric and asymmetric ozone molecules. They found no isotope effect of this sort but concluded with the following statement:[16] "*We speculate that the symmetry effect of Coriolis coupling can appear in quantum mechanical analysis of the model*".

During the past few years, we have undertaken a series of methodological developments and numerical calculations to explore this possibility. In the first two papers of this series,[1,11] we carefully looked at the properties of low-energy coupled rotational−vibrational states in symmetric and asymmetric ozone molecules, including fine details of the ro-vibrational structure, such as parity splitting (Λ-doubling). In the third paper of this series,[2] we extended the vibrational content of our calculations to reach resonances above dissociation threshold, but the full coupled ro-vibrational calculations were only feasible for $J \leq 4$.

However, for the recombination reaction at room temperature, the rotational states of ozone up to $J \sim 50$ need to be included, with largest contributions coming from $J \sim 25$ to 30. Here, using our new partially coupled method, we performed the calculations of scattering resonances for $J = 24$ and $J = 28$ and computed the corresponding partition functions. These data permit us to quantify the magnitude of Coriolis coupling effect for the highly excited rotational states of ozone and the role it plays in the ozone forming reaction. We demonstrate that, overall, the effect of Coriolis coupling is indeed substantial at $J \sim 25-30$, which manifests as an increase of the resonance partition function by up to 20% (for $J = 24$), but we also show that this effect is about the same in symmetric ($^{16}O^{18}O^{16}O$) and asymmetric ($^{18}O^{16}O^{16}O$) ozone molecules, which means that it is unlikely to produce any significant mass-independent symmetry-driven fractionation of oxygen isotopes in the atmosphere.

II. THEORY

All calculations of scattering resonances in this paper have been performed with the SpectrumSDT program, which was recently made available to the community.[17] SpectrumSDT performs calculations in Adiabatically adjusting Principal axis Hyperspherical (APH) coordinates,[18−23] where the Hamiltonian operator can be written as[1,11]

$$\hat{H} = \hat{T}_\rho + \hat{T}_\theta + \hat{T}_\varphi + V_{\text{pes}} + V_{\text{ext}} + \hat{T}_{\text{sym}} + \hat{T}_{\text{asym}} + \hat{T}_{\text{cor}} \tag{1}$$

The first five terms in eq 1 affect only the vibrational degrees of freedom (ρ, θ, and φ), which are treated in the same way as described in ref 11 and do not participate in the rotation−vibration coupling; therefore, we will not discuss them further here. The remaining three terms affect both vibrational and rotational degrees of freedom, but only the asymmetric top rotor term $\hat{T}_{\text{asym}}$ and the Coriolis term $\hat{T}_{\text{cor}}$ are responsible for the rotation−vibration coupling.[1]

Each coupled rotation−vibration wave function in the APH coordinates can be expanded in a basis as

$$F(\rho, \theta, \varphi, \alpha, \beta, \gamma) = \sum_n h_n(\rho) \sum_\Lambda \sum_k c^n_{\Lambda k} X^n_k(\theta, \varphi) \tilde{D}_\Lambda(\alpha, \beta, \gamma) \tag{2}$$

where $\tilde{D}_\Lambda(\alpha,\beta,\gamma)$ are symmetrized Wigner functions of two parities $p = 0$ or 1, obtained as positive or negative superpositions of regular Wigner functions, as discussed in ref 1. Quantum numbers J and M were omitted for clarity. Quantum number Λ labels projections of the total angular momentum J and varies in the range $0 \leq \Lambda \leq J$. Basis functions $h_n(\rho)$ correspond to the DVR of the hyper-radial coordinate ρ (a grid of points ρ_n), whereas $X^n_k(\theta,\varphi)$ represent a set of 2D basis functions for hyper-angles θ and φ (obtained at each ρ_n by using an SDT procedure).[11,24,25] A set of expansion coefficients $c^n_{\Lambda k}$ for each ro-vibrational state is obtained by finding the eigenstates of the Hamiltonian matrix.

Now let us consider a general structure of the Hamiltonian matrix produced by the last three terms of eq 1 in the basis of eq 2. As it was demonstrated in ref 1, only specific combinations of Λ and Λ' result in nonzero elements of the Hamiltonian matrix. Namely, $\hat{T}_{\text{sym}}$ only couples basis functions with the same values of Λ (i.e., within the diagonal blocks of the matrix, $\Lambda' = \Lambda$), while $\hat{T}_{\text{cor}}$ and $\hat{T}_{\text{asym}}$ couple functions with the values of Λ different by ±1 and ±2, respectively (producing the off-diagonal blocks with $\Lambda' = \Lambda \pm 1$ and $\Lambda' = \Lambda \pm 2$). $\hat{T}_{\text{asym}}$ also contributes to one diagonal block with $\Lambda' = \Lambda = 1$. These properties lead to a "block three-diagonal" structure of the Hamiltonian matrix, shown schematically in Figure 1 for the case of $J = 7$ and $p = 1$. Note that it is sufficient to label the blocks with Λ, since the two parities p are independent and the corresponding Hamiltonian matrices are calculated separately.

In the exact fully coupled calculations the value of Λ goes up to J, which implies that the size of the coupled rotation−vibration Hamiltonian matrix can become very large for large values of J. This can represent significant computational difficulties, especially for calculation of scattering resonances, where the presence of a complex absorbing potential (CAP) makes the Hamiltonian matrix non-Hermitian, and a large

https://doi.org/10.1021/acs.jpca.1c03350
J. Phys. Chem. A 2021, 125, 5661−5669

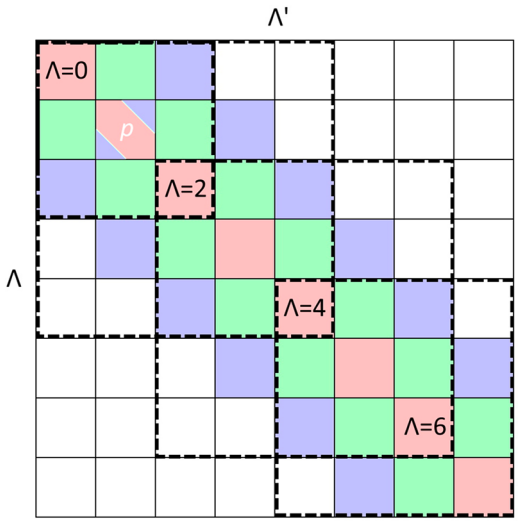

Figure 1. Schematic rotational block structure of the Hamiltonian matrix for $J = 7$ and $p = 1$. Individual blocks are labeled by the values of Λ and Λ' of the symmetric top rotor. Each block includes all vibrational basis functions. Red, green, and blue colors show contributions from $\hat{T}_{sym}$, $\hat{T}_{cor}$, and $\hat{T}_{asym}$ terms in the Hamiltonian operator, respectively. The four black dashed squares show the boundaries of "submatrixes" in the calculations for $\Lambda = 0$, 2, 4 and 6, up to $\Lambda' = \Lambda \pm 2$ in each case. The white p letter marks the only block, where the values of matrix elements are affected by parity.

vibrational basis set is needed to describe delocalized high-energy states above the dissociation threshold. For example, in the case of ozone calculation presented below, the size of each Λ-block is about 20000, which results in the full Hamiltonian matrix of the size about 500000 × 500000 for $J \sim 25$. That is prohibitively expensive to diagonalize.

A well-known straightforward way to make calculations affordable is to neglect all off-diagonal Λ-blocks in the Hamiltonian matrix (due to $\hat{T}_{cor}$ and $\hat{T}_{asym}$ terms of the Hamiltonian operator), in which case the overall matrix splits into the independent diagonal Λ-blocks that can be diagonalized one by one for any value of J. This is called the symmetric top rotor approximation or the Λ-conserving approximation (since Λ becomes a good quantum number). It has been applied extensively in the past to study many molecules and processes, including the kinetics of ozone recombination reaction.[26−31] The effects of neglecting rotation−vibration coupling, and the various methods of improving the accuracy of this approximation, have been recently discussed in detail.[32] But what if the contribution of $\hat{T}_{cor}$ and $\hat{T}_{asym}$ is expected to be important and cannot be neglected?

The two methods described above represent two limiting cases, in which either *all* Λ-blocks are included simultaneously (with the corresponding off-diagonal blocks; the full-coupled exact approach) or only *one* Λ-block is included at a time (symmetric top rotor approximation) in the Hamiltonian matrix. But why not to try an intermediate partially coupled method, in which *some* Λ-blocks of the overall Hamiltonian matrix are included for each Λ? For example, it makes sense to include several nearest blocks in the vicinity of each Λ that are *directly coupled* to it by $\hat{T}_{cor}$ and $\hat{T}_{asym}$, namely $\Lambda' = \Lambda \pm 1$ and $\Lambda' = \Lambda \pm 2$. These are expected to be the most important for a given value of Λ. All other more distant values of Λ', linked by *chain coupling* through these blocks, are expected to be less important and therefore can be neglected. In this way the rotation−vibration coupling is partially included, which justifies the name—a partially coupled method, or a PC-method for short.

Just as in the Λ-conserving approach, in our PC-method a series of independent matrix diagonalizations need to be done for different values of Λ to cover the range of $0 \le \Lambda \le J$. Performing these calculations for all values of Λ up to J, one can obtain a complete spectrum of states for that J. An example of this process is shown in Figure 1, where the borders of reduced "submatrixes" considered for every other value of Λ are shown with dashed lines. Note that the maximum number of Λ-blocks included in each calculation is always limited to five, which makes such calculations affordable even for large values of J.

One feature of this approach is that each submatrix includes a range of Λ values, but only the central value of Λ in each submatrix has its directly coupled blocks; therefore, it is desirable to only take into account contributions from that Λ component. We cannot assign a definite value of Λ to a state, since Λ is not a good quantum number, but we can assign, for each state, a weight equal to the probability in the central Λ. The details of this are further discussed in section III.B (eq 5).

One can view our method in a different way, in terms of the basis set expansion of eq 2. Namely, the symmetric top rotor approximation corresponds to retaining only one expansion term in the sum over Λ, while the fully coupled method uses all terms of expansion up to $\Lambda = J$. The partially coupled method we propose would consider only up to five expansion terms in the range $\Lambda' = \Lambda \pm 2$ for each Λ. This gives more flexibility to the basis set, compared to the symmetric top rotor case, and is less demanding numerically compared to the fully coupled method. Therefore, the PC-method can be thought of as a Λ-dependent truncation of the rotational basis set.

In the literature one can find a description of a somewhat similar approach employed by Schinke and co-workers[33,34] to compute scattering resonances in HCO and HOCl, but their method is different. Namely, for each J they included all blocks of the Hamiltonian matrix in the range $0 \le \Lambda \le \Lambda_{max}$, where the value of Λ_{max} is considered to be a convergence parameter. This approach, first of all, is somewhat too straightforward and is not expected to be numerically feasible for heavy molecules. For example, in the calculations of scattering resonances above dissociation threshold in ozone with $J = 24$ and $J = 28$ presented in the next section, the value of at least $\Lambda_{max} = 18$ would be required, but the inclusion of 18 (19, in the case of parity $p = 0$) Λ-blocks is out of question in the case of ozone, since the calculations with five Λ-blocks are already at the limit of our computing power. Also, note that in the method of Schinke some Λ-blocks are included (fully coupled within a group), while others are completely neglected (even the diagonal blocks with $\Lambda > \Lambda_{max}$ are neglected). Our method adopts a more elegant and flexible truncation, in which every diagonal Λ-block is included in the calculations and affects the properties of states within the range $\Lambda - 2 \le \Lambda' \le \Lambda + 2$ of itself. The value of ± 2 in this approach is required to include both the asymmetric top rotor terms and the Coriolis couplings, but in principle one could include more blocks in each window (e.g., $\Lambda' = \Lambda \pm 3, \pm 4$, etc.), if the computing resources permit.

The accuracy of PC-method for each state depends on the distribution of Λ values in its wave function. Because the range of the Λ states in the truncated basis set is restricted to only

https://doi.org/10.1021/acs.jpca.1c03350
J. Phys. Chem. A 2021, 125, 5661−5669

five ($\Lambda' = \Lambda \pm 2$), the wave functions with much broader distributions would not be accurately described. The actual accuracy of the method is expected to be system/problem dependent and should normally be tested, by comparison with the fully coupled calculations, at least for the low values of J, when the fully coupled calculations are possible. This is what we do next.

III. RESULTS

III.A. Test of PC-Method for Bound States. For the first and the most direct test of the partially coupled method, we performed calculations of several vibrational states (the ground state and the first excited state of each mode) for the rotationally excited $^{16}O^{18}O^{16}O$ with $J = 28$. We focused on $\Lambda = 8$ and considered several levels of theory, with progressively increasing number of Λ-blocks included in the calculations. The results of this convergence study are presented in Figure 2. Specifically, each individual calculation includes all blocks in the range $\Lambda' = \Lambda \pm \Delta\Lambda$, where the value of $\Delta\Lambda$ is varied (progressively increased). When $\Delta\Lambda = 0$, only one block with $\Lambda = 8$ is included, and all couplings with other blocks are disregarded, which corresponds to the symmetric-top rotor limit. The fully coupled limit can be achieved on the other side of the Figure 2, where $\Delta\Lambda$ is large enough to cover all Λ-blocks (which would be $\Delta\Lambda = 20$ in this case, not shown in Figure 2).

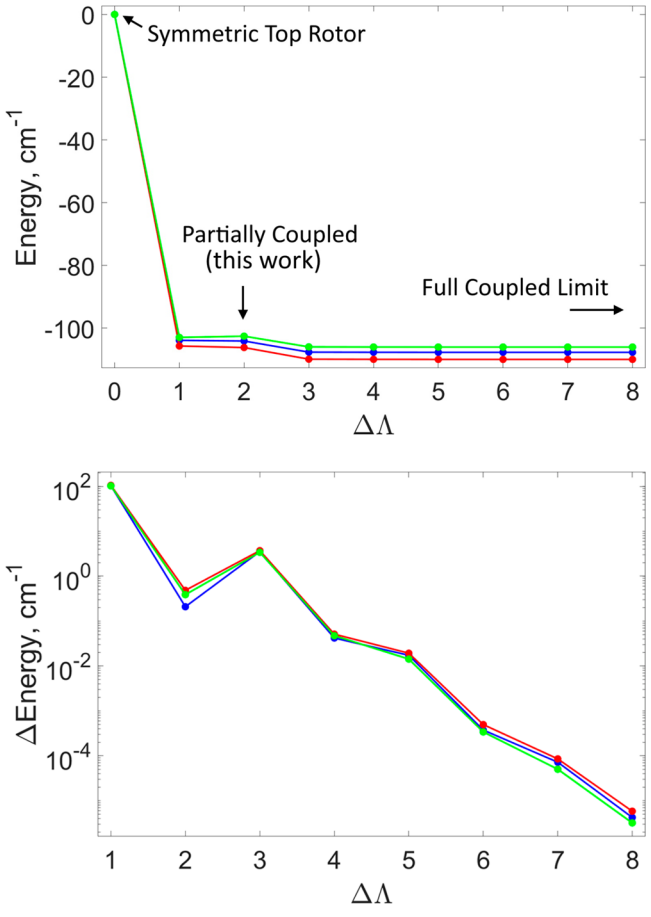

Figure 2. Convergence of energies for three low-lying ro-vibrational states as a function of number of Λ-blocks for $J = 28$ and $\Lambda = 8$. The blue line shows the energy of the ground state. The red and green lines show the energies of vibrationally excited states with one quanta in bending and symmetric stretching modes, respectively. The energies of all states are shown with respect to the energies of symmetric top rotor approximation. The bottom frame shows pairwise differences of the points from the upper frame on logarithmic scale to better visualize energy behavior in the region of large $\Delta\Lambda$.

As one can see from Figure 2, the result of the symmetric top rotor model is way off, by more than 100 cm^{-1}, but inclusion of just one block on each side of $\Lambda = 8$ allows to capture most of the coupling energy. Inclusion of two blocks on each side of $\Lambda = 8$ (which is our partially coupled method, $\Delta\Lambda = 2$) permits to obtain energies converged to within few wavenumbers, which is sufficiently precise for the purpose of our study and for many other practical purposes. Further addition of more Λ-blocks leads to exponential convergence of energy, as can be seen from the bottom frame of Figure 2. Therefore, we conclude that the method works as intended.

Such a direct test of convergence of the individual ro-vibrational states is only feasible at low energies, since it becomes much harder to identify and compare specific states at higher energies, where the spectrum is much denser and states can easily change their relative order. For the highly excited states, such as scattering resonances, it is practical to consider a thermally average property, such as partition function, which is done next.

III.B. Test of PC-Method for Scattering Resonances. Here we are looking at scattering resonances above dissociation threshold that play the role of metastable states (reaction intermediates) in the process of ozone formation. For each state i, we have its energy E_i, width Γ_i, and wave function. From the wave function, we compute the probability p_i for symmetric and asymmetric ozone molecules, by integration over the inner parts of the PES (see the Supporting Information for details), where the metastable ozone states can be quenched by bath gas collisions into a stable ozone molecule below the dissociation threshold. Different resonances possess different properties (E_i, Γ_i, p_i) and make different contributions into the overall recombination process. The thermal average of these contributions is computed and analyzed.

Namely, for the case of symmetric top rotor, we can compute, for each Λ, the following moiety, named the dynamical partition function:

$$Q(\Lambda) = \sum_i w_i p_i \exp\left(-\frac{E_i}{kT}\right) \tag{3}$$

where the summation goes over all scattering resonances. Besides the usual Boltzmann factor, the contribution of each resonance includes its weight w_i and stabilization probability p_i that account for the processes of resonance formation, decay, and quenching. The weight w_i is computed assuming the standard Lindeman mechanism of recombination[35] as $w_i = k_i^{dec}/(k_i^{dec} + k_i^{stab}[M])$, where first-order rate coefficient for spontaneous decay of a resonance is determined by its width, $k_i^{dec} = \Gamma_i/\hbar$, while the second-order rate coefficient for stabilization by bath gas collisions is assumed to be proportional to the probability, p_i.[2,11,31] The bath gas concentration [M] corresponds to the experiments of Mauersberger and co-workers[12] at $P = 267$ hPa (~0.3 bar) and $T = 298$ K.

Note that each factor in eq 3 is unitless and varies between zero and one. Consider two limiting cases: very narrow resonances with $p_i \to 1$ and $w_i \to 0$ (almost bound states) and very broad resonances with $p_i \to 0$ and $w_i \to 1$ (almost free-

https://doi.org/10.1021/acs.jpca.1c03350
J. Phys. Chem. A 2021, 125, 5661−5669

particle states). Neither of these would make a significant contribution to the dynamical partition function Q. Only the resonances with a reasonable combination of probability and width (both p_i and w_i are nonzero) make significant contribution to Q and to the recombination process.

In Figure 3, blue symbols correspond to the dynamical partition function $Q(\Lambda)$ obtained by five independent

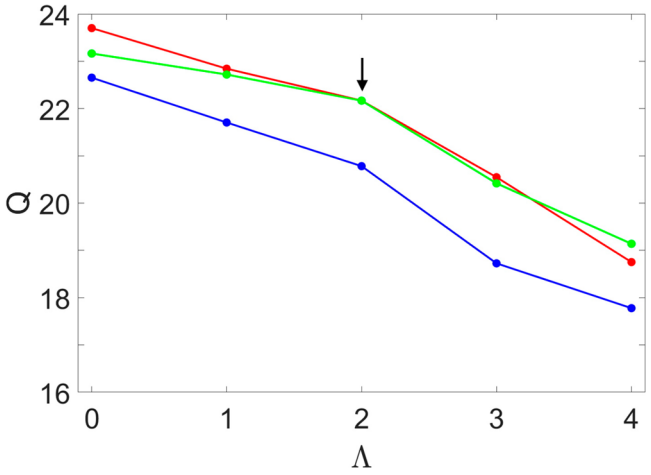

Figure 3. Dynamical partition functions computed for symmetric ozone $^{16}O^{18}O^{16}O$ at $J = 4$ and $p = 0$. Calculations with no coupling (symmetric top) are shown in blue, partial coupling in red, and the full coupling (exact) in green. The black arrow shows the point ($\Lambda = 2$), where the partial coupling approach coincides with the exact method.

calculations with $0 \leq \Lambda \leq 4$ within the symmetric top rotor approximation. The meaning of this partition function is the effective number of scattering resonances populated at given temperature, and we see the numbers on the order of $Q \sim 20$ per Λ. As a function of Λ, the value of Q decreases, which is partially due to the Boltzmann factor (energy of states E_i grows quickly when Λ is raised) and partially due to the weight w_i (higher centrifugal barrier hinders the population of resonances).

Red symbols in Figure 3 correspond to the results of fully coupled calculation. In this case all scattering resonances are determined at once, therefore to compute the individual contribution of each Λ, one has to project it out of the mixed state. This can be done by using the coefficients of expansion in eq 2:

$$a(\Lambda) = \sum_k \sum_n |c^n_{\Lambda k}|^2 \tag{4}$$

where the double sum goes over all vibrational basis functions. Note that $\sum a(\Lambda) = 1$. The amplitude $a(\Lambda)$, computed for each state i, is introduced as another probability factor under the sum in eq 3, which now reads

$$Q(\Lambda) = \sum_i a_i(\Lambda) w_i p_i \exp\left(-\frac{E_i}{kT}\right) \tag{5}$$

From Figure 3 we see that the inclusion of ro-vibrational coupling (red vs blue symbols) leads to the increase of dynamical partition function Q for all values of Λ, in this case by about 5% on average, which is a non-negligible effect.

Green symbols in Figure 3 correspond to the results of our partially coupled method, also processed by using eq 5 to project out the contribution of each Λ. We see that they are much closer to the results of exact fully coupled method compared to the data obtained within the symmetric top approximation. For $\Lambda = 2$ the result of partially coupled calculations coincides with the exact result (marked with an arrow in Figure 3), since in this case the "five-block window" of the partially coupled approach happens to cover the whole Hamiltonian matrix. As we move away from $\Lambda = 2$, the fully and partially coupled approaches start to diverge but still stay close to each other and away from the data of the decoupled symmetric top rotor approximation. The difference is largest for the terminal Λ values ($\Lambda = 0$ and $\Lambda = 4$). Generally, one should expect that the deviation from the fully coupled method is proportional to the number of missing Λ-blocks in a reduced submatrix.

From Figure 3 we conclude that the partially coupled approach behaves as expected and can be used as an approximation for calculation of the coupled rotational−vibrational resonance spectra for large values of J.

III.C. Calculations of Partition Functions at High *J*. In our PC-method the cost of calculations (per Λ) is the same no matter what the value of J is. Of course, larger values of J come with broader range of possible Λ values, but if $Q(\Lambda)$ dependence is smooth, then all values of Λ are not really needed (one can skip some values of Λ and recover this information by interpolation). In this work, to map out the $Q(\Lambda)$ dependencies for $J = 24$ and 28, typical to ozone formation at room temperature,[29] we performed calculations with $\Lambda = 0$, 1, 2, 3, 4, 8, 12, and 16. The results for $J = 28$ are presented here. The results for $J = 24$ are qualitatively similar and are given in the Supporting Information. Because the fully coupled calculations are unaffordable in these cases, only the results for the uncoupled (symmetric top) and for our partially coupled method are presented and discussed.

The two upper frames of Figure 4 represent the $Q(\Lambda)$ dependencies computed for symmetric $^{16}O^{18}O^{16}O$ and asymmetric $^{16}O^{16}O^{18}O$ molecules at $J = 28$. For $\Lambda \geq 1$ the results were averaged over the two parities (for $\Lambda = 0$ only the parity giving even value of $J + p$ is possible). We see again that as Λ is raised, the values of $Q(\Lambda)$ decrease rather monotonically and are expected to vanish around $\Lambda = 20$. One clear trend observed in all these data is that the values of partition function Q are systematically higher in the calculations where the rotation−vibration coupling is included (using our PC-method) compared to the uncoupled (symmetric top rotor) calculations, by up to 17% for $J = 28$ and up to 20% in the case of $J = 24$ (see the Supporting Information). This is expected since the density of states generally increases with additional couplings.

As it was discussed in ref 1, the Hamiltonian matrix for each J and parity (p) breaks down to two independent blocks that correspond to two different ro-vibrational symmetries. For the electronic ground state of ozone (symmetric $^1A_1$) and for the isotopes considered in this work (spinless bosons), only the overall symmetries A_1 and A_2 are allowed for the rotational−vibrational states, while the symmetries B_1 and B_2 are forbidden (see Table 1). The symmetrized rotational basis functions in eq 2 are given by

$$\tilde{D}^{Jp}_{\Lambda M}(\alpha, \beta, \gamma) = \sqrt{\frac{2J+1}{16\pi^2(1+\delta_{\Lambda 0})}} [D^J_{\Lambda M}(\alpha, \beta, \gamma) + (-1)^{J+\Lambda+p} D^J_{-\Lambda M}(\alpha, \beta, \gamma)] \tag{6}$$

https://doi.org/10.1021/acs.jpca.1c03350
J. Phys. Chem. A 2021, 125, 5661−5669

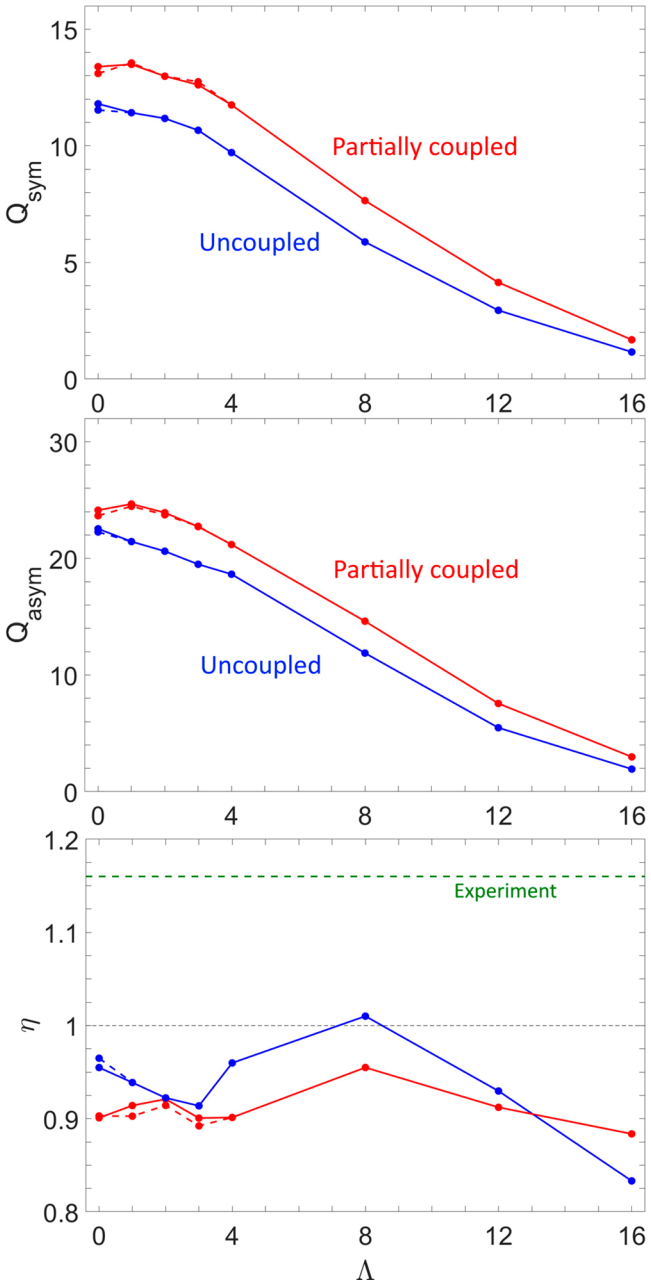

Figure 4. Parity-averaged dynamical partition functions for symmetric (top frame) and asymmetric (middle frame) ozone molecules at J = 28 and the resultant η effect (bottom frame). The blue and red lines correspond to the uncoupled (symmetric top) and partially coupled calculations, respectively. The solid lines are computed by using the states of allowed ro-vibrational symmetry only. The dashed lines correspond to the dynamical partition functions that are also symmetry-averaged and include both allowed and forbidden symmetries.

where the indexes J, p, and M are all indicated explicitly and $D^J_{\Lambda M}$ is a regular Wigner function. As one can see from eq 6, the symmetry of function $\tilde{D}^{Jp}_{\Lambda M}$ is determined by the values of J, p, and Λ. For fixed J and p, the symmetry of $\tilde{D}^{Jp}_{\Lambda M}$ is determined by Λ, and the corresponding allowed vibrational symmetries alternate between A_1 and B_1 as a function of Λ, as demonstrated by Table 1. The solid lines in all frames of Figure 4 are calculated by using the states of allowed symmetry only.

Table 1. Summary of Possible Symmetries of Different Components of Ro-vibrational Wave Functions for Several Small Values of Λ (the Pattern Continues Up to $\Lambda = J$) for Even Values of J[a]

ro-vibrational state symmetry		rotational state			vibrational state symmetry	
allowed	forbidden	parity	Λ	symmetry	allowed	forbidden
A_1	B_1	$p = 0$	0	A_1	A_1	B_1
			1	B_1	B_1	A_1
			2	A_1	A_1	B_1
			3	B_1	B_1	A_1
A_2	B_2	$p = 1$	1	A_2	A_1	B_1
			2	B_2	B_1	A_1
			3	A_2	A_1	B_1
			4	B_2	B_1	A_1

[a]Note that the $\Lambda = 0$ state exists only when $J + p$ is even.

As a computational experiment, we also tried to include the states with forbidden symmetry. The dashed lines in Figure 4 correspond to the $Q(\Lambda)$ averaged over both allowed and forbidden symmetries. One can see that the inclusion of forbidden symmetry does not significantly alter the results, which tells us that the two ro-vibrational symmetries behave similarly and there are no unexpected/unusual isotope effects associated with the forbidden symmetry.

In the case of uncoupled calculations (blue curves in Figure 4) parity p does not affect energies of the ro-vibrational states.[1] For $\Lambda \geq 1$ the states of the two parities are degenerate, and although only one vibrational symmetry is allowed for each parity (see Table 1), both vibrational symmetries show up in the spectrum because they come from different parities. The exception is $\Lambda = 0$, when only one (giving even $J + p$) parity is possible, and thus only one vibrational symmetry is allowed. Therefore, the inclusion of forbidden symmetry makes difference only in the case of $\Lambda = 0$, and this is why solid and dashed blue lines in Figure 4 deviate one from another only at $\Lambda = 0$.

In the coupled ro-vibrational calculations parity affects only one block, labeled by p in Figure 1 (namely, the diagonal block $\Lambda' = \Lambda = 1$). In the fully coupled calculations this block affects all states of the system, but its influence, and the role of parity becomes weaker in the states dominated by large values of Λ. For example, it is known that the value of parity splitting (Λ-doubling) drops exponentially[11] as a function of Λ. Importantly, in our partially coupled method this chain coupling is restricted to act within five blocks, $\Lambda' = \Lambda \pm 2$. Therefore, the calculations for $\Lambda \geq 4$ are decoupled from $\Lambda = 0$ and $\Lambda = 1$, and the states of two parities become degenerate, just as in the uncoupled case, considered above. Thus, solid and dashed red lines in Figure 4 deviate one from another only at $\Lambda \leq 3$.

In this sense, the effects of parity of the rotational functions and the symmetry of vibrational functions are closely related and should be considered together. Our data indicate that they both are relatively small in the rotationally excited ozone molecules (dashed vs solid lines of the same color in Figure 4) compared to the overall effect of the ro-vibrational coupling (red vs blue lines in Figure 4).

III.D. Implications for Symmetry-Driven Isotope Effect. The bottom frame of Figure 4 reports the ratio of dynamical partition functions in symmetric and asymmetric ozone molecules for J = 28 (shown in the two upper frames):

https://doi.org/10.1021/acs.jpca.1c03350
J. Phys. Chem. A 2021, 125, 5661−5669

$$\eta = \frac{Q^{asym}}{2Q^{sym}} \tag{7}$$

The factor of 2 is introduced for convenience to offset the statistical difference in the number of states between the symmetric $^{16}O^{18}O^{16}O$ and asymmetric $^{16}O^{16}O^{18}O$ ozone molecules. The value of the η effect on the order of $\eta = 1.16$ (green in Figure 4) would permit to interpret mass-independent fractionation as a symmetry-driven isotope effect,[12,36] with asymmetric ozone molecules forming 16% faster than the symmetric ones. Note that the experimental line does not represent the actual dependence of the η effect on Λ (which is unknown) and is given for the purpose of comparison with the results of calculations only.

However, the data presented in Figure 4 for all values of Λ, both uncoupled (blue) and partially coupled (red), exhibit the values of η less than 1 (with the exception of one blue point where η is just slightly larger than 1). We can also see that the addition of partial ro-vibrational coupling (red) did not introduce any systematic bias in the favor of asymmetric isotopomer. On average, the value of η-effect remained similar to the uncoupled case (blue). The data presented in the Supporting Information for $J = 24$ are qualitatively similar.

In Figure 5 we present the average values of resonance widths Γ, computed for symmetric and asymmetric ozone molecules for $J = 28$ using the dynamical partition function $Q(\Lambda)$ as a weighting function (as in ref 2). From these data one can conclude that, on average, the inclusion of ro-vibrational coupling has little effect on resonance widths and therefore is not expected to affect the lifetimes of the metastable ozone states. The inclusion of forbidden symmetry, related to the effect of parity, makes even less difference (dashed lines). Resonance widths appear to be more sensitive to the value of Λ, but this effect is about the same in symmetric and asymmetric ozone molecules. Also, comparison of average resonance widths computed here for $J = 24$ and $J = 28$ with those published earlier[2] for $J \leq 4$ shows that they are less sensitive to J and more sensitive to Λ, but again, these dependencies are very similar in symmetric and asymmetric ozone molecules, which does not help us to explain why the asymmetric ozone molecules are formed faster.

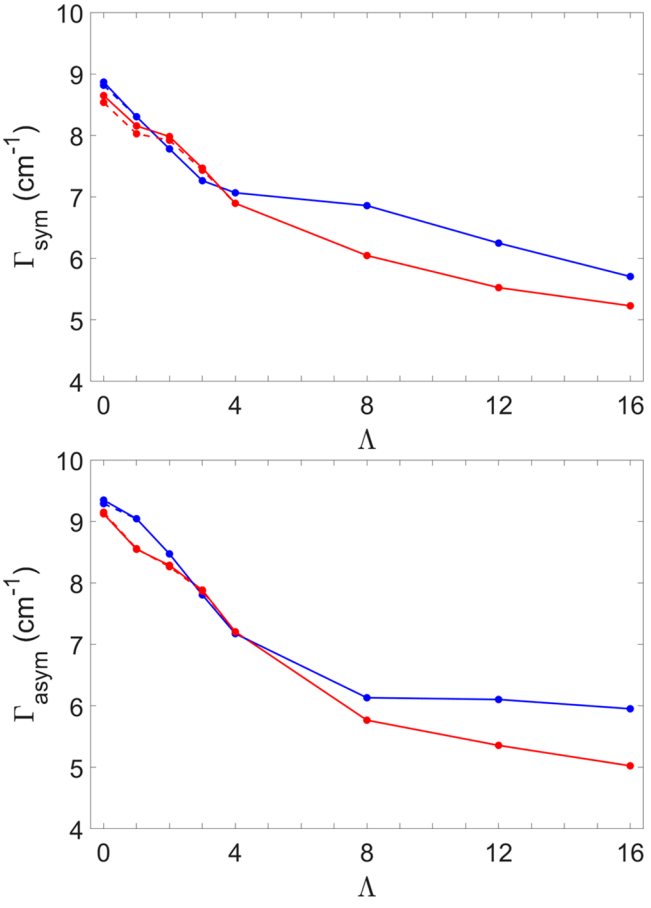

Figure 5. Average values of resonance widths in symmetric (top frame) and asymmetric (bottom frame) ozone molecules for $J = 28$. The meaning of lines and colors is the same as in Figure 4.

IV. CONCLUSIONS

In this paper we were able to quantify the effect of rotation−vibration coupling on resonance spectra of ozone isotopomers with very large values of J. In particular, our goal was to determine whether rotation−vibration coupling (Coriolis effect) could introduce a systematic bias in favor of isotopically substituted asymmetric isotopomers of ozone, such as $^{16}O^{16}O^{18}O$, since this could help to explain the origin of the mysterious η effect, responsible for mass-independent fractionation of oxygen isotopes in the atmosphere.

We found that addition of the ro-vibrational coupling has little effect on the average widths (decay rates) of the metastable ozone states for $J = 24$ and $J = 28$. Their lifetimes remain similar in symmetric and asymmetric ozone molecules, with or without inclusion of the ro-vibrational coupling. We also found that the ro-vibrational coupling appreciably increases the average number of metastable ozone states (given by the dynamical partition function), but these changes are rather uniform through symmetric and asymmetric isotopomers of ozone. On the basis of the results presented here, we conclude that the rotation−vibration coupling is not expected to be responsible for a robust symmetry-driven isotope effect.

To make these calculations numerically feasible, we developed a partially coupled method that permits to capture the major contribution of ro-vibrational coupling terms without diagonalization of the entire Hamiltonian matrix. This method is approximate, but it is general and applicable to many other molecules and processes in the spectroscopic and dynamic context. The number of coupled Λ-blocks does not have to be equal to five, as in this paper ($\Lambda' = \Lambda \pm 2$). Instead, it can be viewed as a convergence parameter, varied to achieve desired level of accuracy. Moreover, if the z-axis is chosen perpendicular to the molecular plain, which results in a two-diagonal block structure of the Hamiltonian matrix,[1] then the number of directly coupled rotational blocks can be reduced to just three. This would make the method even more affordable, enabling the coupled rotation−vibration calculations for more complicated systems and processes.

■ ASSOCIATED CONTENT

Supporting Information

The Supporting Information is available free of charge at https://pubs.acs.org/doi/10.1021/acs.jpca.1c03350.

Section A: technical details of the calculations; section B: results for $J = 24$; section C: a symmetry table analogous to Table 1, but for the case of odd values of J;

https://doi.org/10.1021/acs.jpca.1c03350
J. Phys. Chem. A 2021, 125, 5661−5669

section D: a description of the archive file with all data calculated for this paper (PDF)

The ro-vibrational states calculated for this paper. Please, refer to section D of the Supporting Information for a more detailed description (ZIP)

AUTHOR INFORMATION

Corresponding Author

Dmitri Babikov − *Department of Chemistry, Marquette University, Milwaukee, Wisconsin 53201-1881, United States;* orcid.org/0000-0002-4667-7645; Email: dmitri.babikov@mu.edu

Author

Igor Gayday − *Department of Chemistry, Marquette University, Milwaukee, Wisconsin 53201-1881, United States;* orcid.org/0000-0002-3950-3356

Complete contact information is available at: https://pubs.acs.org/10.1021/acs.jpca.1c03350

Author Contributions

I.G. contributed to methodology, software development, data acquisition, visualization, data analysis, and writing; D.B. contributed to supervision, methodology, data analysis, and writing.

Notes

The authors declare no competing financial interest.

ACKNOWLEDGMENTS

This research was supported by the NSF AGS program Grant AGS-1920523. This research used resources of the National Energy Research Scientific Computing Center (NERSC), a U.S. Department of Energy Office of Science User Facility located at Lawrence Berkeley National Laboratory, operated under Contract DE-AC02-05CH11231. I.G. was supported by MolSSI Investment Fellowship, funded by NSF ACI-1547580.

REFERENCES

(1) Gayday, I.; Teplukhin, A.; Kendrick, B. K.; Babikov, D. Theoretical Treatment of the Coriolis Effect Using Hyperspherical Coordinates, with Application to the Ro-Vibrational Spectrum of Ozone. *J. Phys. Chem. A* **2020**, *124*, 2808−2819.

(2) Gayday, I.; Grushnikova, E.; Babikov, D. Influence of the Coriolis Effect on the Properties of Scattering Resonances in Symmetric and Asymmetric Isotopomers of Ozone. *Phys. Chem. Chem. Phys.* **2020**, *22*, 27560−27571.

(3) Petty, C.; Spada, R. F. K.; Machado, F. B. C.; Poirier, B. Accurate Rovibrational Energies of Ozone Isotopologues up to J = 10 Utilizing Artificial Neural Networks. *J. Chem. Phys.* **2018**, *149*, 024307.

(4) Chen, W.; Poirier, B. Quantum Dynamical Calculation of All Rovibrational States of HO_2 for Total Angular Momentum J = 0−10. *J. Theor. Comput. Chem.* **2010**, *09*, 435−469.

(5) Brandon, D.; Poirier, B. Accurate Calculations of Bound Rovibrational States for Argon Trimer. *J. Chem. Phys.* **2014**, *141*, 034302.

(6) Yang, D.; Hu, X.; Zhang, D. H.; Xie, D. An Improved Coupled-States Approximation Including the Nearest Neighbor Coriolis Couplings for Diatom-Diatom Inelastic Collision. *J. Chem. Phys.* **2018**, *148*, 084101.

(7) Pack, R. T. Space-fixed vs Body-fixed Axes in Atom-diatomic Molecule Scattering. Sudden Approximations. *J. Chem. Phys.* **1974**, *60*, 633−639.

(8) McGuire, P.; Kouri, D. J. Quantum Mechanical Close Coupling Approach to Molecular Collisions. j_z-conserving Coupled States Approximation. *J. Chem. Phys.* **1974**, *60*, 2488−2499.

(9) Parker, G. A.; Pack, R. T. Identification of the Partial Wave Parameter and Simplification of the Differential Cross Section in the j_zCCS Approximation in Molecular Scattering. *J. Chem. Phys.* **1977**, *66*, 2850−2853.

(10) Parker, G. A.; Pack, R. T. Rotationally and Vibrationally Inelastic Scattering in the Rotational IOS Approximation. Ultrasimple Calculation of Total (Differential, Integral, and Transport) Cross Sections for Nonspherical Molecules. *J. Chem. Phys.* **1978**, *68*, 1585−1601.

(11) Gayday, I.; Teplukhin, A.; Kendrick, B. K.; Babikov, D. The Role of Rotation−Vibration Coupling in Symmetric and Asymmetric Isotopomers of Ozone. *J. Chem. Phys.* **2020**, *152*, 144104.

(12) Janssen, C.; Guenther, J.; Mauersberger, K.; Krankowsky, D. Kinetic Origin of the Ozone Isotope Effect: A Critical Analysis of Enrichments and Rate Coefficients. *Phys. Chem. Chem. Phys.* **2001**, *3*, 4718−4721.

(13) Thiemens, M. H. History and Applications of Mass-Independent Isotope Effects. *Annu. Rev. Earth Planet. Sci.* **2006**, *34*, 217−262.

(14) Thiemens, M. H.; Chakraborty, S.; Dominguez, G. The Physical Chemistry of Mass-Independent Isotope Effects and Their Observation in Nature. *Annu. Rev. Phys. Chem.* **2012**, *63*, 155−177.

(15) Kryvohuz, M.; Marcus, R. A. Coriolis Coupling as a Source of Non-RRKM Effects in Ozone Molecule: Lifetime Statistics of Vibrationally Excited Ozone Molecules. *J. Chem. Phys.* **2010**, *132*, 224305.

(16) Kryvohuz, M.; Marcus, R. A. Coriolis Coupling as a Source of Non-RRKM Effects in Triatomic near-Symmetric Top Molecules: Diffusive Intramolecular Energy Exchange between Rotational and Vibrational Degrees of Freedom. *J. Chem. Phys.* **2010**, *132*, 224304.

(17) SpectrumSDT; https://github.com/IgorGayday/SpectrumSDT.

(18) Pack, R. T.; Parker, G. A. Quantum Reactive Scattering in Three Dimensions Using Hyperspherical (APH) Coordinates. Theory. *J. Chem. Phys.* **1987**, *87*, 3888−3921.

(19) Teplukhin, A.; Babikov, D. Interactive Tool for Visualization of Adiabatic Adjustment in APH Coordinates for Computational Studies of Vibrational Motion and Chemical Reactions. *Chem. Phys. Lett.* **2014**, *614*, 99−103.

(20) Teplukhin, A.; Babikov, D. Visualization of Potential Energy Function Using an Isoenergy Approach and 3D Prototyping. *J. Chem. Educ.* **2015**, *92*, 305−309.

(21) Kendrick, B. K.; Pack, R. T.; Walker, R. B.; Hayes, E. F. Hyperspherical Surface Functions for Nonzero Total Angular Momentum. I. Eckart Singularities. *J. Chem. Phys.* **1999**, *110*, 6673−6693.

(22) Kokoouline, V.; Lapierre, D.; Alijah, A.; Tyuterev, V. G. Localized and Delocalized Bound States of the Main Isotopologue $^{48}O_3$ and of ^{18}O-Enriched $^{50}O_3$ Isotopomers of the Ozone Molecule near the Dissociation Threshold. *Phys. Chem. Chem. Phys.* **2020**, *22*, 15885−15899.

(23) Alacid, M.; Leforestier, C. The Role of Rotation in the Calculated Ultraviolet Photodissociation Spectrum of Ozone. *J. Chem. Phys.* **2001**, *114*, 1685−1692.

(24) Bačić, Z.; Whitnell, R. M.; Brown, D.; Light, J. C. Localized Representations for Large Amplitude Molecular Vibrations. *Comput. Phys. Commun.* **1988**, *51*, 35−47.

(25) Light, J. C.; Carrington, T. Discrete-Variable Representations and Their Utilization. In *Advances in Chemical Physics*; Prigogine, I., Rice, S. A., Eds.; John Wiley & Sons: 2000; Vol. *114*, pp 263−310.

(26) Teplukhin, A.; Babikov, D. Efficient Method for Calculations of Ro-Vibrational States in Triatomic Molecules near Dissociation Threshold: Application to Ozone. *J. Chem. Phys.* **2016**, *145*, 114106.

(27) Teplukhin, A.; Babikov, D. A Full-Dimensional Model of Ozone Forming Reaction: The Absolute Value of the Recombination

Rate Coefficient, Its Pressure and Temperature Dependencies. *Phys. Chem. Chem. Phys.* **2016**, *18*, 19194−19206.
(28) Teplukhin, A.; Babikov, D. Several Levels of Theory for Description of Isotope Effects in Ozone: Symmetry Effect and Mass Effect. *J. Phys. Chem. A* **2018**, *122*, 9177−9190.
(29) Teplukhin, A.; Gayday, I.; Babikov, D. Several Levels of Theory for Description of Isotope Effects in Ozone: Effect of Resonance Lifetimes and Channel Couplings. *J. Chem. Phys.* **2018**, *149*, 164302.
(30) Teplukhin, A.; Babikov, D. Properties of Feshbach and "Shape"-Resonances in Ozone and Their Role in Recombination Reactions and Anomalous Isotope Effects. *Faraday Discuss.* **2018**, *212*, 259−280.
(31) Gayday, I.; Teplukhin, A.; Babikov, D. The Ratio of the Number of States in Asymmetric and Symmetric Ozone Molecules Deviates from the Statistical Value of 2. *J. Chem. Phys.* **2019**, *150*, 101104.
(32) Sarka, J.; Poirier, B.; Szalay, V.; Császár, A. G. On Neglecting Coriolis and Related Couplings in First-Principles Rovibrational Spectroscopy: Considerations of Symmetry, Accuracy, and Simplicity. II. Case Studies for H_2O Isotopologues, H^+_3, O_3, and NH3. *Spectrochim. Acta, Part A* **2021**, *250*, 119164.
(33) Weiß, J.; Schinke, R.; Mandelshtam, V. A. Renner−Teller Induced Photodissociation of HCO in the First Absorption Band: Determination of Linewidths for the $\tilde{A}^2A''$ K = 0,1 States by Filter-Diagonalization. *J. Chem. Phys.* **2000**, *113*, 4588−4597.
(34) Hauschildt, J.; Weiß, J.; Schinke, R. Influence of Vibrational Resonances and Coriolis Coupling on Dissociation Rates in the Near-Threshold Unimolecular Fragmentation of HOCl. *Z. Phys. Chem.* **2000**, *214*, 609−623.
(35) Babikov, D.; Grushnikova, E.; Gayday, I.; Teplukhin, A. Four Isotope-Labeled Recombination Pathways of Ozone Formation. *Molecules* **2021**, *26*, 1289.
(36) Janssen, C.; Marcus, R. A. Does Symmetry Drive Isotopic Anomalies in Ozone Isotopomer Formation? *Science (Washington, DC, U. S.)* **2001**, *294*, 951a−951.

https://doi.org/10.1021/acs.jpca.1c03350
J. Phys. Chem. A 2021, 125, 5661−5669